



# Improving Dye Wastewater Treatment with a Unique Silver, Carbon Co-doped TiO<sub>2</sub> Absorbent

Feng Chen<sup>1</sup>, Guiyang Yan<sup>1,3\*</sup>, Liuping Zheng<sup>2,4</sup>, Qingshan Pan<sup>2</sup>, Zongxuan Hong<sup>1</sup>,  
Lishan Xie<sup>2</sup>, Yingying Huang<sup>2</sup>

<sup>1</sup>Department of Chemistry, Ningde Normal University, Ningde, Fujian, 352100, China

<sup>2</sup>College of Chemistry and Chemical Engineering, Fujian Normal University, Fuzhou, Fujian, 350007, China

<sup>3</sup>Research Institute of Photocatalysis, State Key Laboratory of Photocatalysis on Energy and Environment, Fuzhou, Fujian, 350002, China

<sup>4</sup>Fujian Key Laboratory of Polymer Materials, Fuzhou 350007, P. R. China

Received 27 Sept 2014, Revised 19 Feb 2015, Accepted 19 Feb 2015

\*E-mail: [gyfjnu@163.com](mailto:gyfjnu@163.com)

## Abstract

Silver, carbon-doped TiO<sub>2</sub> absorbent was obtained using hydrothermal method with titanium sulfate as a titanium source. Reactive brilliant red X-3B was used as a target degradation material to evaluate its adsorption activity. Physicochemical properties of the absorbent was characterized by analytical techniques such as XRD, SEM-EDS, TG-DTG, TEM-HRTEM, BET, and XPS. The results showed that the synthesized samples has a phase of anatase with typical mesoporous structure, and it also has a good adsorption activity of reactive brilliant red X-3B. The Ag-C-TiO<sub>2</sub> (calcined at 500°C) absorbent's discoloration rate for reactive brilliant red X-3B (50 ppm) reached 97% after adsorption for 60minutes at absorbent of 1.5 g/L(50 ppm reactive brilliant red X-3B solution), and solution pH of 7~9. This type of Ag-C co-doped TiO<sub>2</sub> could potentially be used as absorbent for dye wastewater treatment based on its unique physicochemical properties.

**Keywords:** absorbent; co-doped; TiO<sub>2</sub>; reactive brilliant red X-3B; performance characterization

## 1. Introduction

With the development of modern industry, environmental pollution is becoming increasingly serious. Dye wastewater appears in many areas with large quantities, and it greatly damages the ecological environment [1]. Some treatment technologies have been used to process dye wastewater, such as activated carbon adsorption, chemical coagulation, microwave radiation and etc. [2,3]. However, the porosity and specific surface area of the activated carbon decrease sharply after activated carbon being used for several times. The regeneration of activated carbon is complicated, therefore the cost of this method is quite high. The chemical coagulation method produces a lot of sediment, which is hard to dehydrate. Microwave radiation method is significantly influenced by the polarity of the wastewater and the effect is little in the low polar or nonpolar wastewater. In general, these methods also have other disadvantages such as requiring large treatment area, complex process, high cost, etc. Therefore, seeking economical and efficient methods for dye wastewater treatment is one of the most important tasks of scientists.

In recent years, TiO<sub>2</sub> is considered to be a preferable photocatalyst in the treatment of dye wastewater, but is rarely used as an absorbent. At present it has been known that TiO<sub>2</sub> was only used as the main component of

composite absorbents for adsorption of heavy metal ions [4] and methylene chloride [5]. The study of co-doped TiO<sub>2</sub> modified absorbent is seldom reported.

This paper reports that silver, carbon co-doped TiO<sub>2</sub> absorbent was obtained using hydrothermal method with titanium sulfate as a titanium source. Reactive brilliant red X-3B was used as a target degradation material to evaluate the adsorption activity of this type of absorbent. The structural characteristics of the absorbent were analyzed via XRD, SEM-EDS, TG-DTG, TEM-HRTEM, BET and XPS for further understanding of its physical-chemical properties.

## 2. Experimental

### 2.1. Preparation of absorbents

A designed amount of AgNO<sub>3</sub> and glucose were first dissolved in 60 mL deionized water. 5 g of Ti(SO<sub>4</sub>)<sub>2</sub> was then added into the above solution with continuous stirring at room temperature. After continued mixing for about 1 h, the mixture was transferred into a PTFE-lined reactor, and was reacted for 12 h at the temperature of 180 °C. The precipitate was filtrated, followed by washing, drying, porphyzation. Finally, the sample is calcined for 2 h at a designed calcination temperature. The Ag-C-TiO<sub>2</sub> absorbent powder was then obtained. To find the optimum preparation condition, we examined the effect of various calcination temperatures and ratios of doping compounds respectively. As a comparison, the pure TiO<sub>2</sub> absorbent, silver-doped TiO<sub>2</sub> absorbent, and carbon doped TiO<sub>2</sub> absorbent were obtained using the same method.

### 2.2 Evaluation of the absorbent activity

Reactive brilliant red X-3B was used as a target degradation material to evaluate the adsorption activity of the absorbent materials. This method is commonly used to measure the efficiency of dye wastewater treatment [6]. 0.06 g of absorbent was dispersed in a 40 mL solution of reactive brilliant red X-3B at a designed concentration. After a certain time, a sample of the solution was taken and centrifuged. The supernatant liquid was taken and the absorbance of the liquid was measured. The activity of absorbent is evaluated by the discoloration of brilliant red X-3B. The calculation is as follows:

$$\text{Discoloration rate (D\%)} = \frac{A_0 - A}{A_0} \times 100\%$$

where A<sub>0</sub> and A stand for the absorbance values of dye before and after reaction.

### 2.3 Characterization of absorbents

**XRD:** Philips company X'PertMPD powder diffractometer was used to analyze the phase of the Ag-C-TiO<sub>2</sub> absorbent, with 40 kV tube voltage and 40 mA tube current (Cu K<sub>α</sub> radial, λ=0.154 nm, scanning area 2θ=10–80°, scanning range 2°/min). **SEM:** JEOL company JSM-7500F scanning electron microscope was used to analyze the surface morphology of the specimen, with a 5.0 kV acceleration voltage, 15 keV X-ray energy and 1000 times magnification. **TG-DTG:** The TA company SDTQ600 thermal Analyzer was used, with nitrogen flow of 70 mL/min, heating rate of 10 °C/min and temperature range of 28–895 °C. **BET:** Coulter instrument company Omnisorp100CX adsorption was used with static adsorption method at liquid nitrogen temperature (77K). **TEM-HRTEM:** FEI company's G20 electron microscope was used to analyze the specimen at the voltage of 75 kV. **XPS:** VG MultiLab2000 spectrometer was used with the Mg K<sub>α</sub> X-ray emission sources.

## 3. Results and analysis

### 3.1 Evaluation of adsorption activity

#### 3.1.1 The influence of calcination temperature

Fig.1 shows the effect of the sample calcination temperature of absorbent Ag-C-TiO<sub>2</sub> on their activities for degrading reactive red X-3B with 1.5 g/L of Ag-C-TiO<sub>2</sub> added to 50 ppm reactive red X-3B solution and 1 h of

dark reaction. According to Fig. 1, the adsorption activity first increases as the sample calcination temperature increases to 500°C, and then starts to decrease as the sample calcination temperature continues to increase over 500°C. Sample calcination temperature of 500°C appears to be the optimum calcination temperature. High-temperature calcination may change the crystal form of TiO<sub>2</sub> and make the absorbent sintering, thus decreasing the adsorption activity and the discoloration rate of the reactive red X-3B.[7]

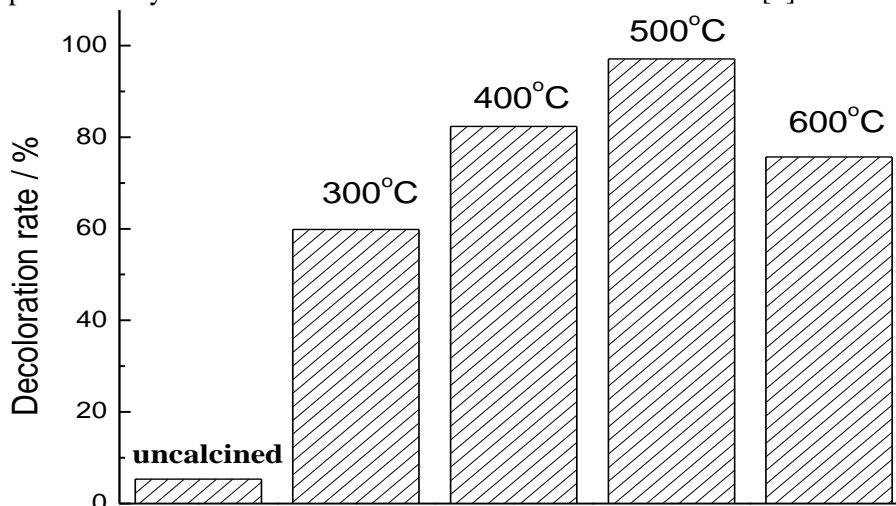


Figure 1: The effect of calcination temperature of Ag-C-TiO<sub>2</sub> on the adsorption properties.

### 3.1.2 The influence of doping ratio

Fig. 2 shows the relationship of molar ratio of Ag to C of the Ag-C-TiO<sub>2</sub> with the decoloration rate with 1.5 g/L of Ag-C-TiO<sub>2</sub> added to 50 ppm reactive red X-3B solution and 1 h of dark reaction. We chose various Ag-C ratios, such as 0.05-0.1, 0.1-0.3, 0.2-0.5, 0.1-0.7, 0.2-0.8, 0.3-0.7, and the results manifest that the absorbent has the best adsorption effect when the optimal Ag-C doping ratio is 0.2-0.8. Excessive doping components are easy to enrich on the surface of the absorbent, which results in the decrease of the effective interactive surface area of the absorbent with reactive red X-3B, and in turn the decrease in the adsorption activity [8].

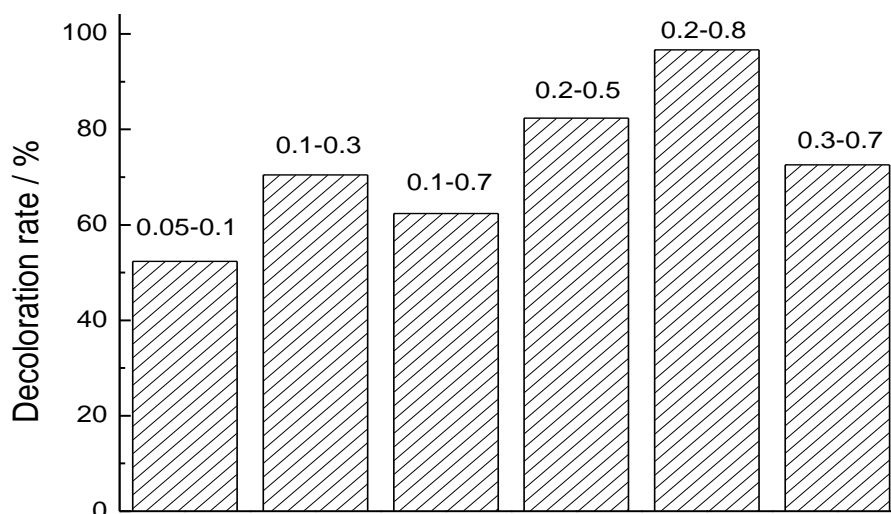
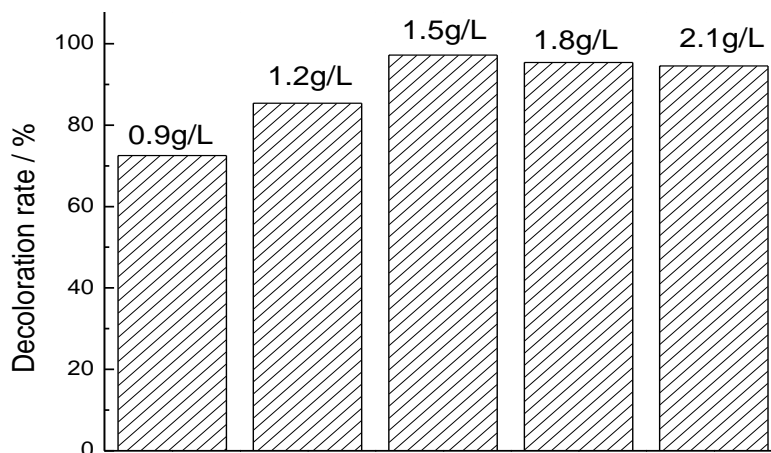


Figure 2: The effect of different molar ratio of Ag to C of Ag-C-TiO<sub>2</sub> on the decoloration rate.

### 3.1.3 The influence of the absorbent usage

Fig. 3 shows the activity diagram for the effect of amount of Ag-C-TiO<sub>2</sub> added (prepared at calcination temperature of 500°C) on the decoloration rate of 50 ppm activated red X-3B solution at 1 h of dark reaction. When the amounts of absorbent added to the solution are 0.9, 1.2, 1.5, 1.8, 2.1 g/L, the discoloration rates of activated red X-3B are 72.55, 85.37, 97.21, 95.38, 94.55 % respectively. Taking consideration of both discoloration rates and costs, we chose the optimum consumption of the absorbent in this system to be 1.5 g/L. Excess amount of absorbent addition to solution may cause shielding, condensation and settlement, leading to the slightly decrease in the adsorption activity [9].



**Figure 3:** The effect of the amount of Ag-C-TiO<sub>2</sub> (prepared at calcination temperature of 500°C) used on the decolorization rate.

### 3.1.4 The influence of the acidity of the reactant

Fig.4 shows the effect of acidity of the reactant solution on the decoloration rate of 50 ppm activated red X-3B solution at 1 h of dark reaction. Fig.4 indicates that the acidity and basicity have a significant influence on the rates of degradation of reactive red X-3B. The adsorption rate is high under neutral and alkaline conditions, while the adsorption rate is low under acidic condition. The possible reason is that the surface of the absorbent has positive charge in the acidic condition, which goes against the adsorption of the dye reactive red X-3B with negative charge on the surface, resulting in the decrease of adsorption efficiency as well as the degradation of reactive red X-3B.

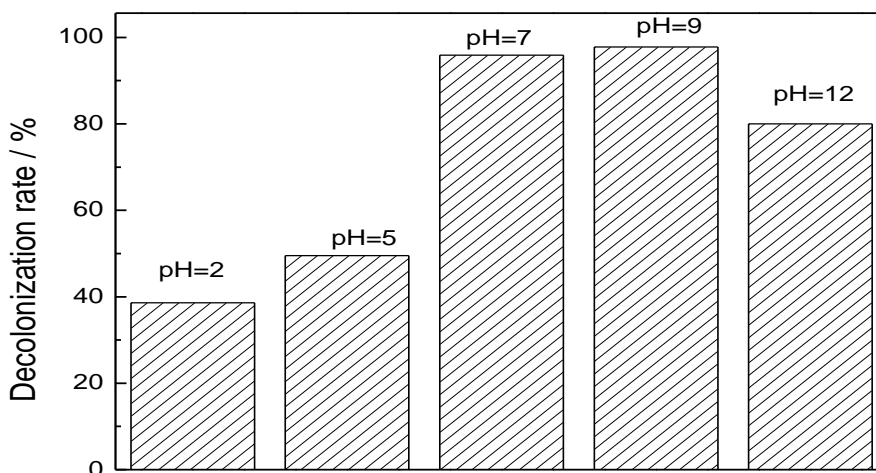


**Figure 4:** The effect of different pH value of the reactant on the discoloration rate of Ag-C-TiO<sub>2</sub>.

### 3.2 Characterization of the Absorbent

#### 3.2.1 XRD

Fig. 5 is the XRD spectra of the Ag-C-TiO<sub>2</sub> samples calcined at various temperatures for precursors prepared in optimized preparation conditions. From the graph we can see clearly that the characteristic absorption peaks of Ag element [10]. The peak at about 27° may belong to the characteristic absorption peak of C element, which coincides with that of anatase TiO<sub>2</sub> [11]. With the increase of calcination temperature, the half-width of the main peak in the samples decreases, indicating that the sizes of crystal grain grow with the elevated calcination temperature. Comparing the experimental results, we can see that the characteristic peak of rutile TiO<sub>2</sub> appears after the calcination at 600 °C, and it is no longer anatase phase. The adsorption activity relates to the purity of anatase phase, which is in accordance with the results of the 2.1.1. In addition, high calcination temperature may result in sintering of the absorbent, thus leading to the decrease of the adsorption activity.

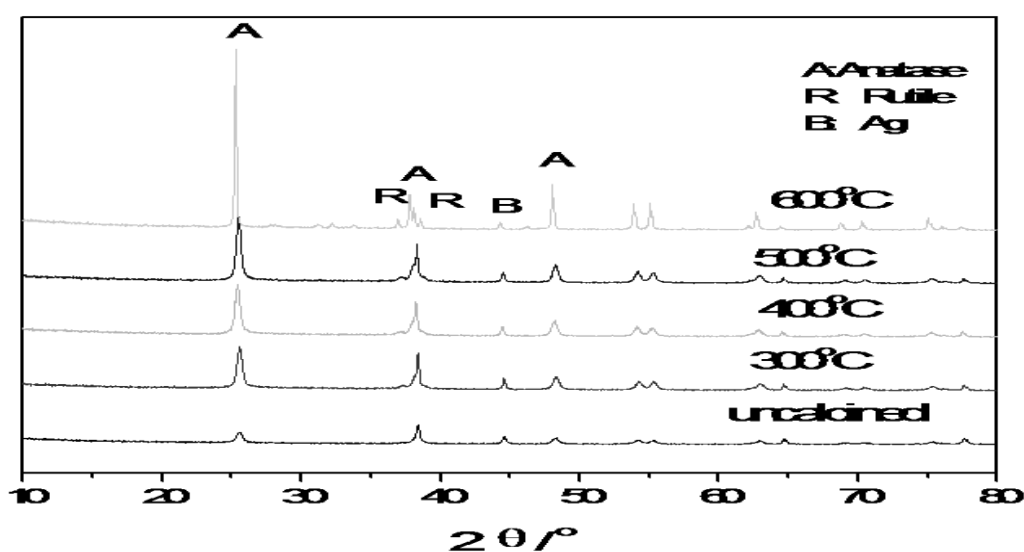


Figure 5: XRD spectra of Ag-C-TiO<sub>2</sub> calcined at various temperatures

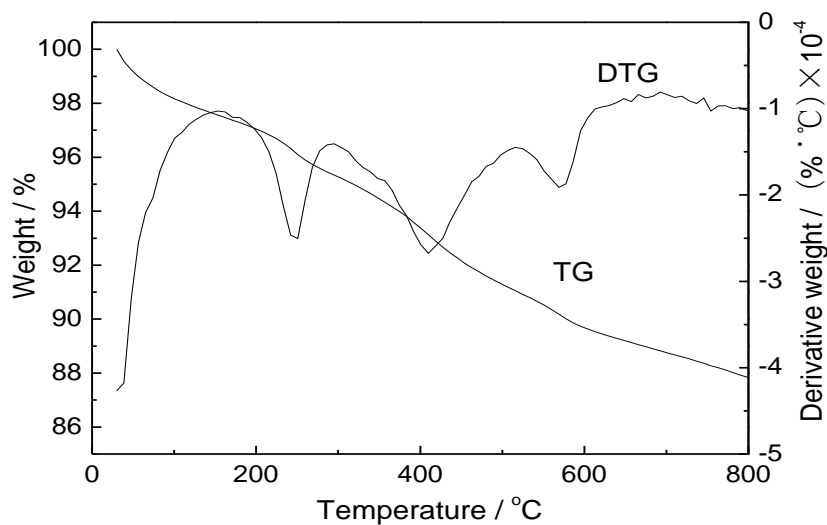
#### 3.2.2 TG-DTG

Fig.6 shows the TG-DTG spectra of Ag-C-TiO<sub>2</sub>. With the increase of temperature, the mass loss rate is relatively constant, and the total mass loss rate is 12.6 %. From the curves of the TG-DTG, it is manifested that there are three heat effect peaks. The peak at about 250 °C is mainly associated to the desorption of the adsorbed water and surfaced adsorbed organic compounds on the sample. The peak at about 400 °C is probably caused by the decomposition of adsorbed AgNO<sub>3</sub> on the sample surface, and the peak at about 600 °C is probably caused by the phase change of TiO<sub>2</sub> from anatase to rutile phase.

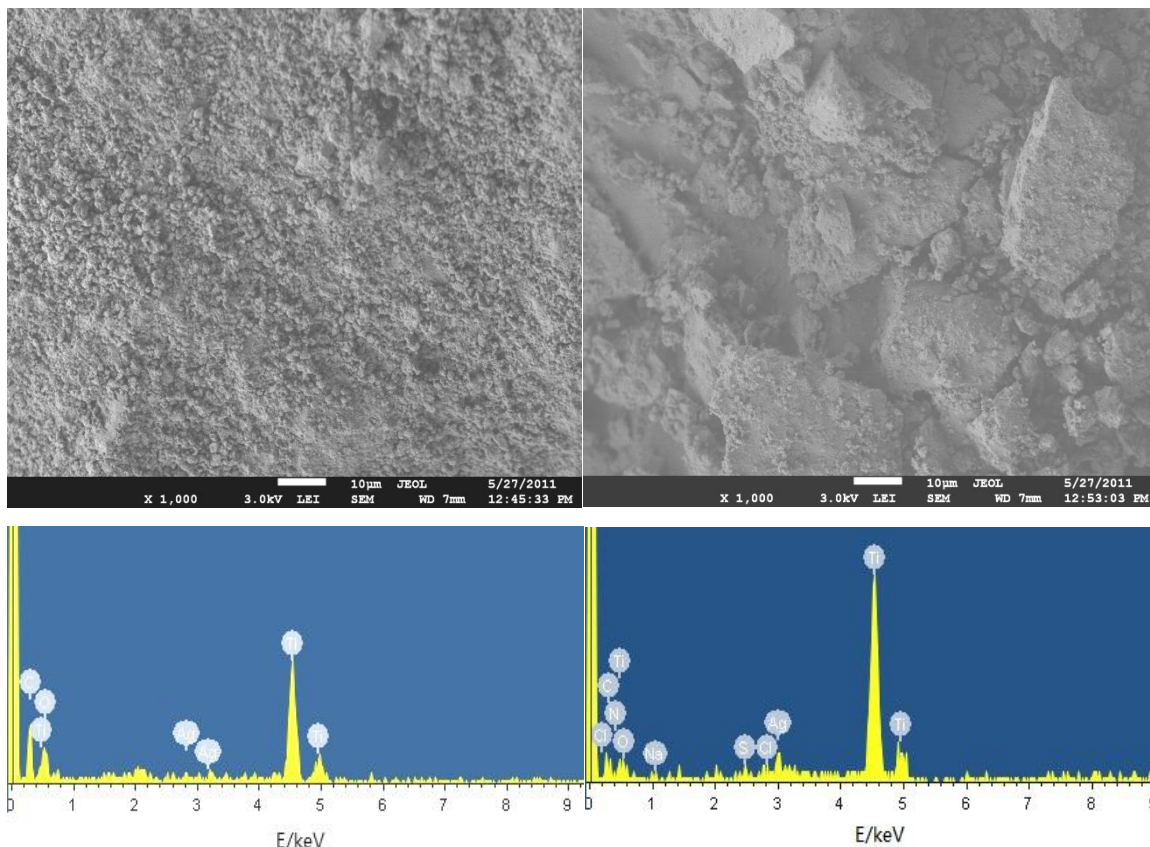
#### 3.2.3 SEM-EDS

Fig.7 is the SEM and EDS micrograph of Ag-C-TiO<sub>2</sub> absorbent before and after adsorption of reactive red X-3B. From Fig.7, the volume of the absorbent apparently increased after the adsorption, which was about tens of times larger than that before the adsorption. Combined with EDS energy spectrum analysis, it is obvious that Ag and C are presented in the specimen, suggesting that Ag-C co-doped TiO<sub>2</sub> has been synthesized. At the same time, elements of S and Cl that are in the characteristics structure of reactive brilliant red X-3B are also observed from the EDS spectrum, suggesting that reactive brilliant red X-3B has been adsorbed successfully.

According to the datum of the EDS, we can estimate the Ti/Ag/C ratio in the Ag-C-TiO<sub>2</sub> to be about 1:0.012:0.89, which is close to the ratio of n(Ti):n(Ag):n(C) of 1:0.015:0.90 in the original material preparation.



**Figure 6:** TG-DTG spectra of Ag-C-TiO<sub>2</sub>.



**Figure 7:** SEM and EDS micrograph of Ag-C-TiO<sub>2</sub> before (left) and after (right) adsorption.

### 3.2.4 BET

Fig. 8 shows the BJH pore size distribution (left) and N<sub>2</sub> adsorption-desorption isotherms (right) of TiO<sub>2</sub> and Ag-C-TiO<sub>2</sub> respectively. As is shown, the synthetic TiO<sub>2</sub> and Ag-C-TiO<sub>2</sub> are ascribed to nanomaterial and their pore sizes are about 8 nm, both of typical mesoporous structure. The specific surface area of the Ag-C co-doped TiO<sub>2</sub> is larger than that of pure TiO<sub>2</sub>, with pure TiO<sub>2</sub> specific surface area of 43.53 m<sup>2</sup>g<sup>-1</sup> and Ag-C-TiO<sub>2</sub> specific surface area of 52.68 m<sup>2</sup>g<sup>-1</sup> respectively.

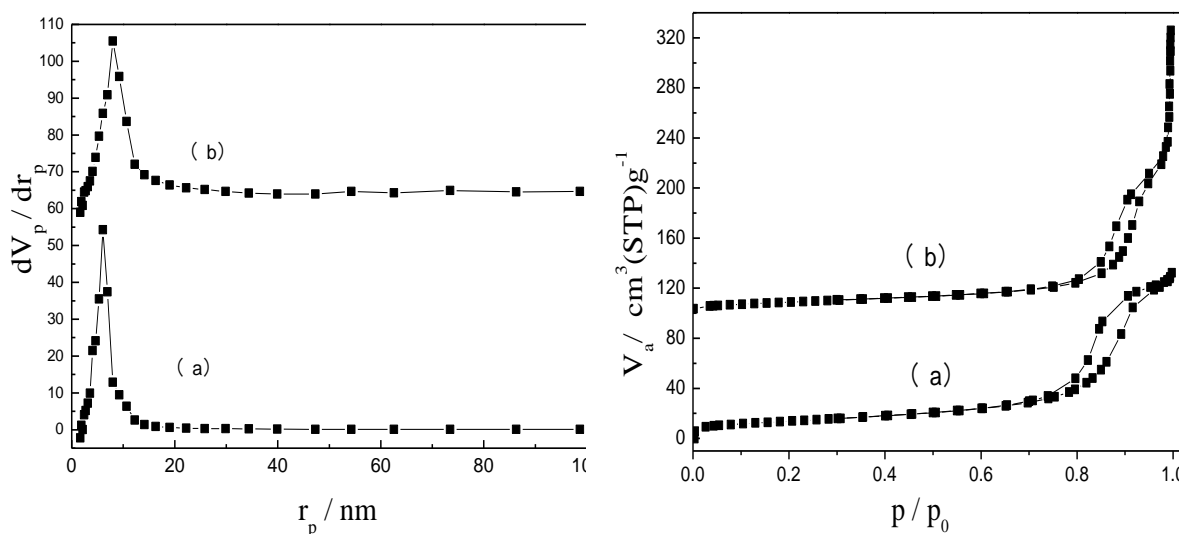


**Figure 8:** The BJH pore size distribution (left) and  $\text{N}_2$  adsorption-desorption isotherms (right) of  $\text{TiO}_2$  and  $\text{Ag-C-TiO}_2$ . (a)  $\text{TiO}_2$ ; (b)  $\text{Ag-C-TiO}_2$ .

### 3.2.5 TEM-HRTEM

The TEM and HRTEM images of  $\text{Ag-C-TiO}_2$  are shown in Fig.9. Some interplanar distances observed from the images are 0.25 nm and 0.35 nm respectively. These values correspond to the same interplanar distances of (004) and (001) planes of typical  $\text{TiO}_2$  anatase phase. The results demonstrate that the synthetic  $\text{Ag-C-TiO}_2$  absorbent is anatase phase, in agreement with the analysis results of XRD. Some darker areas are observed in which the interplanar distance (0.30 nm) is assigned to C-Ti [12] and the other interplanar distance (1.6 nm) is ascribed to  $\text{Ag}_2\text{O}$  (220). Combined with results of XPS, the presence of  $\text{Ag}_2\text{O}$  is verified. The size of the synthetic  $\text{Ag-C-TiO}_2$  absorbent is uniform and at about 5 nm, which in general is in consistency with the measurement from BET.

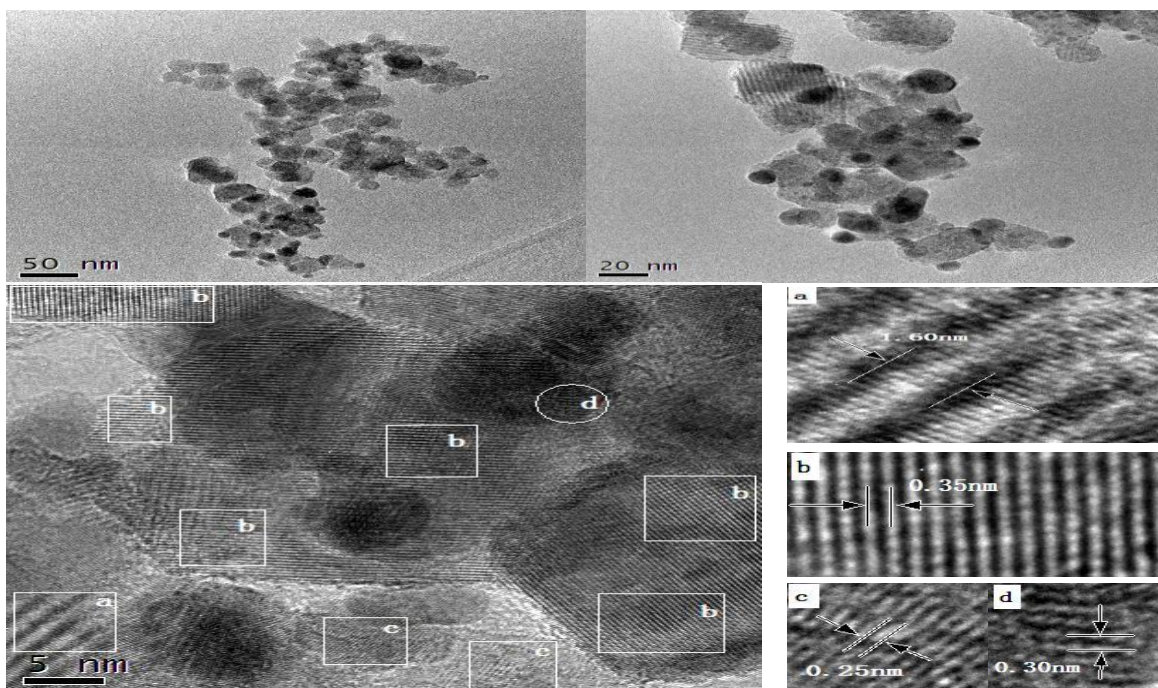


**Figure 9.** TEM and HRTEM of  $\text{Ag-C-TiO}_2$ .

### 3.2.6 XPS

Fig. 10 is the XPS full spectrum of specimens. In the spectrum, the spectral peaks of all the elements are clearly visible. The ratio of Ti/O is 1:2 in the TiO<sub>2</sub> sample. Based on the sensitivity factors and the binding energy and peak area of the characteristic elements in the sample (Table.1), the atomic number of Ti/O/Ag/C is estimated to be 1:2.82:1.36:0.31. This result implies that there may exist some other oxides in the specimens.

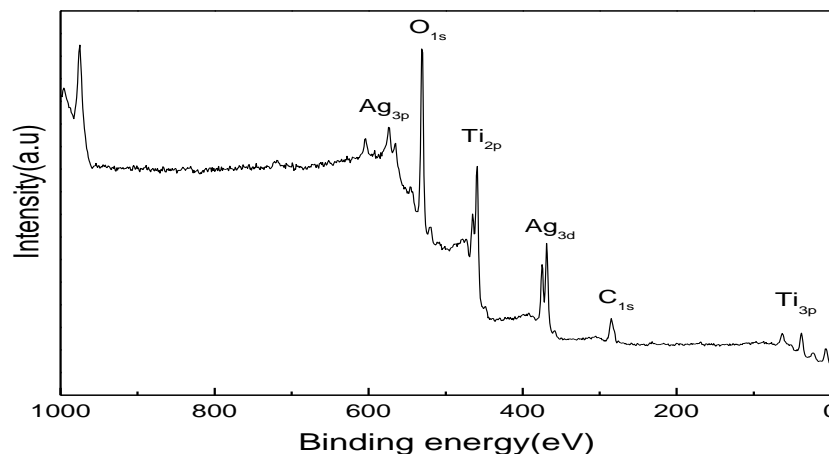


**Figure 10:** XPS survey scan spectra of Ag-C-TiO<sub>2</sub>.

**Table 1:** The sensitivity factor, banding energy and peak area of characteristic peaks of all of the elements

	O <sub>1s</sub>	Ti <sub>2p</sub>	Ag <sub>3d</sub>	C <sub>4f</sub>
sensitivity factor	2.93	7.91	18.04	1
banding energy	529.98	458.67	364	156.5
peak area	10452	100868	71519	17611
	7			

With respect to carbon from XPS spectra of C<sub>1s</sub> (Fig.11), there are three different components contributed to the C<sub>1s</sub> peak. The first component, at 285.1eV, is ascribed to SP<sup>2</sup> hybridization; while thesecond component, located at 288.6eV, is related to chemisorped CO<sub>2</sub> and CO on the surface of the sample. Finally, the third component, at 281.2eV, is generated from the C-Ti bond. These results show that the TiO<sub>2</sub> had been successfully blended with C. [13].

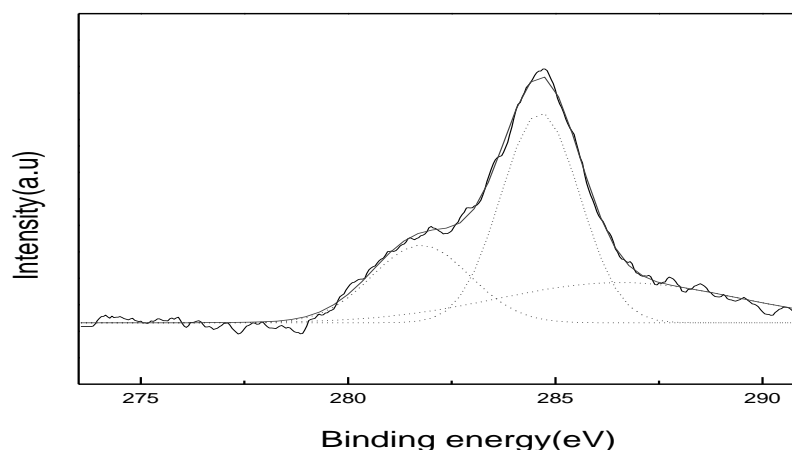


**Figure 11:** XPS survey scan spectra of C<sub>1s</sub>.

From the XPS spectra of Ti (Fig.12), two different peaks at 458.6eV and 464.3eV contribute to the  $Ti_{2p}$  peak, with  $Ti_{2p_{3/2}}$  located at 458.6eV and the  $Ti_{2p_{1/2}}$  located at 464.3eV. The shapes of the  $Ti_{2p_{3/2}}$  and the  $Ti_{2p_{1/2}}$  XPS lines indicate that the Ti is present only as  $Ti^{4+}$ . [14]

From the XPS spectra of  $Ag_{3d}$  (Fig.13), the first peak, at 374 eV, was assigned to the  $Ag_{3d_{5/2}}$ , while the second one, at 368.1 eV, was assigned to the  $Ag_{3d_{3/2}}$ . This result demonstrated that the Ag may be present as  $Ag_2O$  [15], and this assumption is also verified from the results in Table.1. However, from the fact that there was little displacement between the  $Ag_2O$  and Ag [16], we still need more evidence to determine this inference accurately.

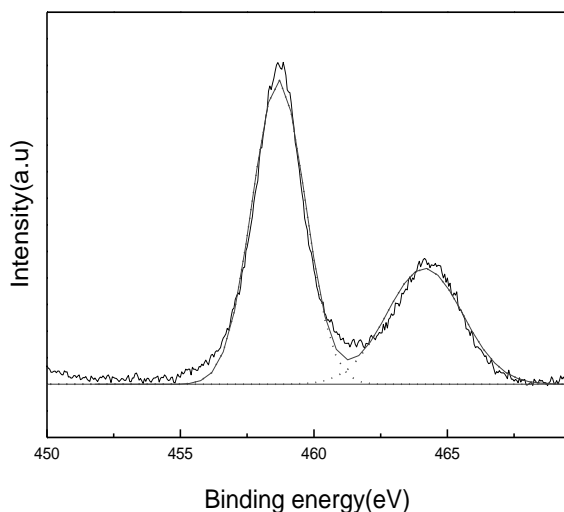


**Figure 12:** XPS survey scan spectra of  $Ti_{2p}$ .

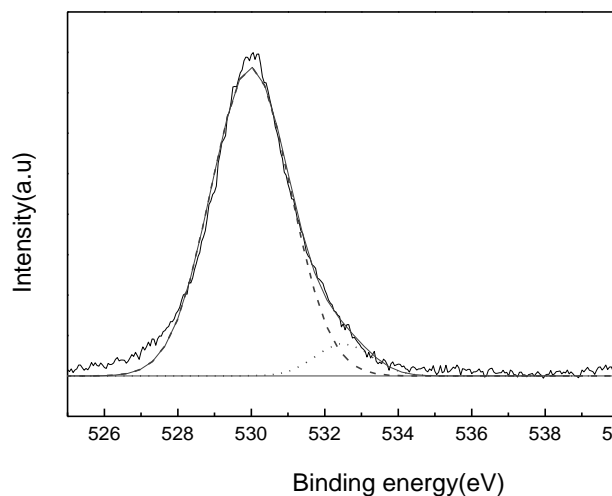


**Figure 13:** XPS survey scan spectra of  $Ag_{3d}$ .

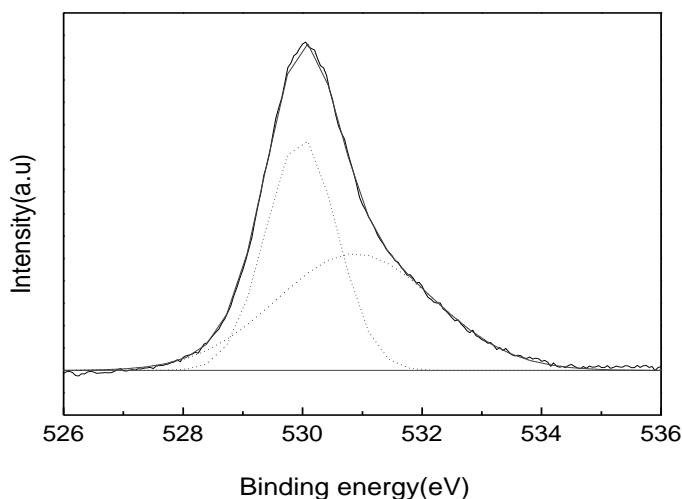


**Figure 14:** De-convoluted XPS spectra of  $O_{1s}$ .

Fig.14 is the XPS spectra of  $O_{1s}$  in the specimens. Asymmetric peak shape in the Fig.14 demonstrates that there are different kinds of the element O. Generally, the existing forms of O include  $O^{2-}$ ,  $OH^-$  and  $O_{ads}$ . However,  $O^{2-}$  and  $O_{ads}$  were proposed mainly from the peak fitting process. The peak at 529.98 eV is close to the binding energy of  $O_{1s}$  in  $Ag_2O$  (530.3 eV) [17], which further demonstrated the presence of  $Ag_2O$ . In addition,

the peak located at the higher binding energy might be assigned to  $O_{ads}$  or OH. These two existing forms of O have strong oxidation power in the adsorption and light catalytic reaction process, and in turn could enhance the activity of adsorption and light catalysis.

## Conclusion

In this study, Ag-C-TiO<sub>2</sub> absorbent is synthesized by hydrothermal method and the material shows good adsorption activity. Physical and chemical characterization of the structure shows that the sample has typical sharp anatase structure, and it belongs to nanometer materials. The particle size of this absorbent is about 8 nm. Silver element exists in the form of Ag<sub>2</sub>O, while carbon element exists in bonding with titanium element. The preliminary experimental results show that the decoloration rate of the reactive brilliant red X-3B could reach 97% with the conditions of sample calcination temperature of 500°C, the dosing quantity at 1.5 g/L and the pH of the solution in the range of 7-9.

**Acknowledgment**-We are grateful to the National Natural Science Foundation of China (Grant No. 21473096), the Ningde Normal University projects on serving the western coast to the TW strait (Grant No. 2010H103), and the Project of Fujian Province Communications Department (Grant No. 201323).

## References

1. Wadley S. L. S., Gillham R. W., Gui L. *Ground Water* 43 (2005) 9.
2. Lalhrualtuanga H., Jayaram K., Prasad M. N.V., Kumar K. K. *J. Hazard. Mater.* 175 (2010) 311.
3. Du F., Fischer J. E., Winey K. I. *J. Polym. Sci. Part B: Polym. Phys.* 41 (2003) 3333.
4. Kim H. T., Lee C. H., Shul Y. G., Moon J. K., Lee E. H. *Separ. Sci. Technol.* 38 (2003) 695.
5. Li S., Zhou P., Ding L. *J. Water Resource & Protection* 3 (2001) 448.
6. Yan G., Zheng L., Xie L., Weng X., Ye J., *Rare Metals* 30 (2011) 259.
7. Huang M., Xu C., Wu Z., Huang Y., Lin J., Wu J. *Dyes Pigments* 77 (2008) 327.
8. Yang X., Cao C., Hohn K., Erickson L., Maghirang R., Hamal D., Klabunde K. *J. Catal.* 252 (2007) 296.
9. Herrmann J. M. *Catal. Today* 53 (1999) 115.
10. Oliveiri G., Ramis G., Escibano V. S. *J. Mater. Chem.* 12 (1993) 1239.
11. Hishiyama Y., Inagaki M., Kimura S. *Carbon* 12 (1974) 249.
12. Banerji A., Relf W. *J. Mater. Sci.* 29 (1994) 1958.
13. Darwan D., Browning J., Gong L. *ACI Mater. J.* 6 (2008) 622.
14. Roy S., Viswanath B., Hegde M. S., Madras G. *J. Phys. Chem. C* 115 (2011) 112.
15. Perkin-Elmer Corporation, *PHI5300 Instrument Manual*, U.S.A., (1988).
16. Voll V. A. *Semiconduct.* 29 (1995) 1081.
17. Blackstock J. J., Donley C. L., Stickle W. F., Ohlberg D. A. A., Yang J. J., Stewart D. R., Williams R. S., *J. Am. Chem. Sci.* 130 (2008) 4041.

(2015) ; <http://www.jmaterenvirosci.com>